Prepared for submission to JHEP

Study of Muon Lifetime and determining the Fermi Coupling constant

Tarkan Yzeiri, Dávid Puskás, Dylan Patel, Indra Gankhuyag

University College London (UCL),
Gower St, Bloomsbury, London WC1E 6BT

E-mail: tarkan.yzeiri.18@ucl.ac.uk, david.puskas.18@ucl.ac.uk, dylan.patel.18@ucl.ac.uk, indra.gankhuyag.18@ucl.ac.uk

Abstract: In this experiment we utilise equipment consisting of a scintillator, a photomultiplier tube with a high voltage setting, and an electronic box that contains a discriminator and time setup. The equipment can be calibrated to detect muon decays by utilising the high voltage and discriminator to obtain the same scintillator flux as the muon density at sea level. Only three of the five obtained muon lifetime measurements $t_2 = (2.13 \pm 0.08)$ µs, $t_3 = (2.1 \pm 0.1)$ µs, and $t_5 = (2.15 \pm 0.07)$ µs agree with the positive muon lifetime value $\tau^+ = (2.1969811 \pm 0.0000022)$ µs [1]. Where the latter measurement had an improved scintillator flux value from a simulation. One of the obtained values $t_1 = (1.92 \pm 0.07)$ µs is an outlier that suggests we measured some other particle decay that skewed the data. All of the experimentally obtained values are lower than the accepted value which is due the equipment detecting both positive and negative muons, where the event of muon capture can skew the experimental lifetime values to be lower than the accepted value. This skew carries over to the respective Fermi Coupling constant values $\frac{G_F}{(\hbar c)^3} = (1.18 \pm 0.02) \times 10^{-5}$ GeV^{-2}, $\frac{G_F}{(\hbar c)^3} = (1.18 \pm 0.03) \times 10^{-5}$ GeV^{-2}, and $\frac{G_F}{(\hbar c)^3} = (1.17 \pm 0.02) \times 10^{-5}$ GeV^{-2} that are all higher than the accepted value of $\frac{G_{Facc}}{(\hbar c)^3} = (1.1663787 \pm 0.0000006) \times 10^{-5}$ GeV^{-2}. The results could be further improved by taking into account a better scintillator flux value and allowing the equipment to detect muon for a longer time.

[1]Word Count: 3328. Excluding title, names, and references.

Contents

1 Introduction

The top of the Earth's atmosphere is bombarded by a flux of cosmic rays [3] that collide with the nuclei of air molecules to produce a shower of particles. One such particle, the pion, then decays into a muon [4] which then further decays into other fundamental particles via the weak force.

$$\mu^+ \rightarrow e^+ + \nu_e + \bar{\nu_\mu} \tag{1.1}$$

$$\mu^- \rightarrow e^- + \bar{\nu_e} + \nu_\mu \qquad \mu^- + p \rightarrow n + \nu_\mu \tag{1.2}$$

Where (1.1) shows positive muon decay and (1.2) shows negative muon decays both via the weak force.

Muon decay is characterised by the following equation:

$$N_\mu(t) = Ae^{-\frac{t}{t_\mu}} + B \tag{1.3}$$

Where $N_\mu(t)$ is the muon population at a time t, t_μ the mean muon lifetime, and A, B constants to be determined.

The strength of the weak force, which is determined by the value of the Fermi coupling constant G_F, can then be calculated by measuring the positive muon lifetime, τ_μ and utilising the following relationship [2]:

$$G_F = \sqrt{\frac{192\pi^3\hbar^7}{\tau_\mu m_\mu^5 c^4}} \tag{1.4}$$

Where m_μ is muon mass and c the speed of light.

2 Equipment

The process of muon decay can be detected using the TeachSpin muon apparatus (Figure 1). Muons entering the detector hit the scintillator which causes it to emit light that can go through the PMT converting the light emitted into an electrical signal that can then be detected. If the same muon then decays in the scintillator, the resulting particle will produce a second signal. The sensitivity of the PMT can be altered by changing its voltage (from HV power). These two signals then enter an electronic box, where the pair of signals are amplified and pass through a discriminator which filters out signals below a threshold voltage. This combined with the changing PMT sensitivity allows us to eliminate background radiation. The initial signal then triggers an FPGA timer in the circuit that lasts 20 µs. If a second signal is detected within this time frame the timer is stopped and the time interval is recorded. If a second signal is not detected within 20 µs then the timer is reset. The time interval data from the FPGA timer is then fed to a PC which contains a muon-shortcut program that can plot a histogram of muon lifetime data.

Note that the accepted positive muon lifetime is $\tau^+ = (2.1969811 \pm 0.0000022)$ µs [1] and number of muon decays follow (1.3). This means that only a small amount of data points will be neglected due to the timer cut off at 20 µs, as exponentially fewer muons have a longer lifetime.

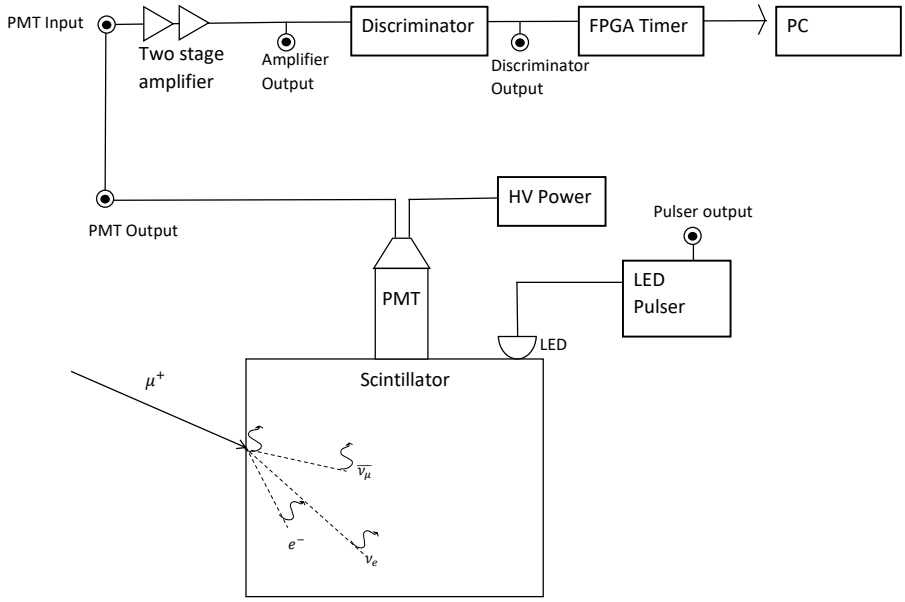

Figure 1. Circuit diagram of the TeachSpin apparatus utilising a detection cylinder consisting of a scintillator, photomultiplier tube (PMT), LED pulser and a HV power supply, connected to an electronic box via the PMT output to PMT input.

3 Methodology

Before the initial study of muon lifetime begins, all the equipment used must be calibrated. This includes studying the effect of the two stage amplifier with varying frequencies of signals that directly corresponds to muon lifetime, verifying whether the FPGA timer can accurately determine the time between two signals, and determining muon flux in order to remove background radiation from our data.

In order to determine the effect of the two stage amplifier, multiple gain values will have to be calculated for varying frequencies. This can be done by first replicating Figure 2 and ensuring the function generator (JUPITER 2000 0.2 Hz - 2 MHz Function Generator) produces sinusoidal waves with amplitude 100 mV.

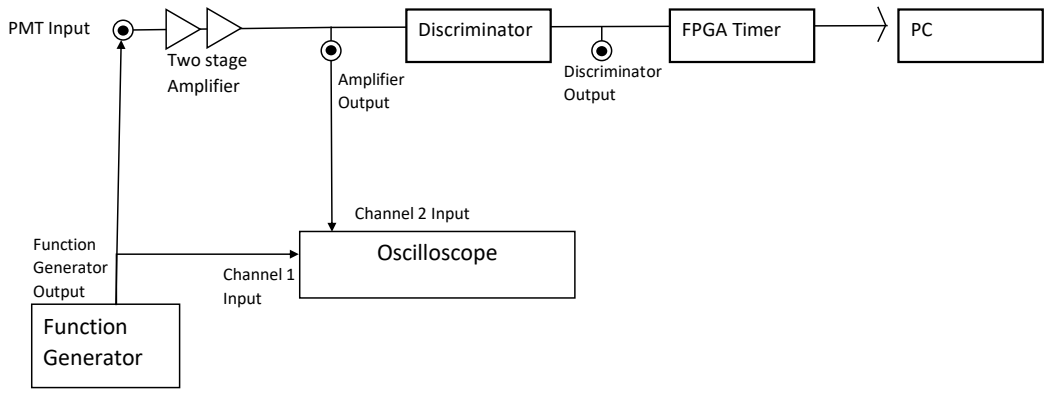

Figure 2. Schematic diagram for determining effect of two stage amplifier. Where oscilloscope (Gw INSTEK GDS-1102A Digital storage oscilloscope) inputs are the function generator outputs before (channel 1) and after (channel 2) the signal has been amplified by the two stage amplifier in the electronic box.

For frequencies which correspond to times around the 20 µs timer cap (50 kHz) and higher, calculate gain by using the oscilloscope to measure the peak to peak voltages of the sinusoidal waves before V_i and after V_{amp} amplification. Where the Gain $G(f)$ of an amplifier:

$$G(f) = \frac{V_{amp}}{V_i} \tag{3.1}$$

Ideally a constant gain would be wanted for the corresponding 0 - 20 µs frequency range, so that signals will be amplified the same amount. This ensures that the same percentage of muon decay signals are passing through the discriminator after they have been amplified. This constant gain will result in an exponential pattern following (1.3).

In order to verify the FPGA timer, its time measurements of the LED pulser will be compared to the same time measurements made by the oscilloscope. This can be done by setting up the equipment according to Figure 5 and first eliminating background radiation by setting the LED pulse width to be greater than the FPGA reset (20 µs), meaning that any concurrent measurements made in the FPGA will be due to background radiation and can be eliminated by raising the discriminator voltage accordingly. The LED pulser can then be set to emit two pulses with a time delay in the range of 0 - 20 µs, which can then be measured by both the FPGA timer and oscilloscope. Where the oscilloscope measures time intervals by calculating the pulse width between the two signals. These two time measurements can then be compared to verify the accuracy of the FPGA timer by plotting a linear line of best fit.

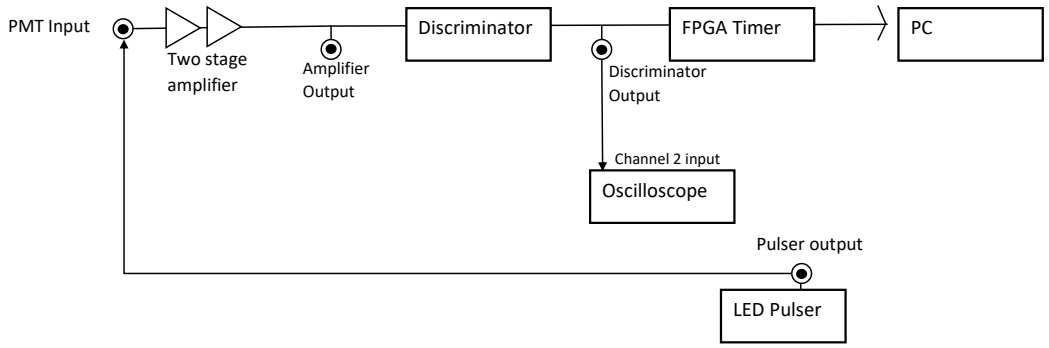

Figure 3. Schematic diagram for verifying FPGA timer. Where FPGA timer results can be accessed in the muon program on the PC and then compared to oscilloscope time interval values.

Calculating a muon flux value allows us to know how many muons hit the scintillator per second. This will allow us to then alter our PMT and threshold voltages such that our equipment detects the same amount of collisions per second in the scintillator as the muon flux, thus allowing us to have more confidence that we are detecting muons and not background radiation. It is also better to have an underestimate as we will then detect fewer muons compared to overestimating, where you will also get background radiation.

For our initial expected muon flux value we only considered muons hitting the top of the scintillator (right circular cylinder of height 12.5 cm and diameter 15 cm). Where a value of intensity of horizontal detection of muons $I = 1\ \mathrm{cm}^{-2}\,\mathrm{min}^{-1}$ [1] is used. This allows us to calculate an initial estimate for muon flux value

$$\Phi_{est} = IA = 2.95\,\mathrm{s}^{-1} \tag{3.2}$$

in the scintillator, where A is the area of the top cylinder.

Once this initial muon flux value is obtained, the equipment can be calibrated to detect the same amount of collisions per second in the scintillator as the initial muon flux value. This can be done by following Figure 1 and allowing the equipment and muon-shortcut program to run for a short amount of time. The muon-shortcut program will then output a 'number of incident muons' (n) value and an 'elapsed time' (t) value which can be used to calculate the average rate of muons per second in the scintillator (or scintillator flux Φ_S) in the equipment:

$$\Phi_S = \frac{n}{t} \tag{3.3}$$

The HV and discriminator voltage can be adjusted accordingly to obtain a value of scintillator flux that is closer to the initial muon flux value. Repeat the above process until a satisfactory value of detection flux is obtained.

Now that the equipment is fully calibrated, the collection of muon decay data can begin. Continuing from the last calibration in obtaining a satisfactory scintillator flux, note down the HV and discriminator voltages used. In order to start taking data click on the 'calibrate' button and select the number of bins to be shown on the plotted histogram. The number of bins can be optimally chosen later when extracting the data and plotting on another external program. After this let the equipment run for about 88 hours and collect data. Due to time constraints we could only have data runs last a select amount of time.

4 Results and analysis

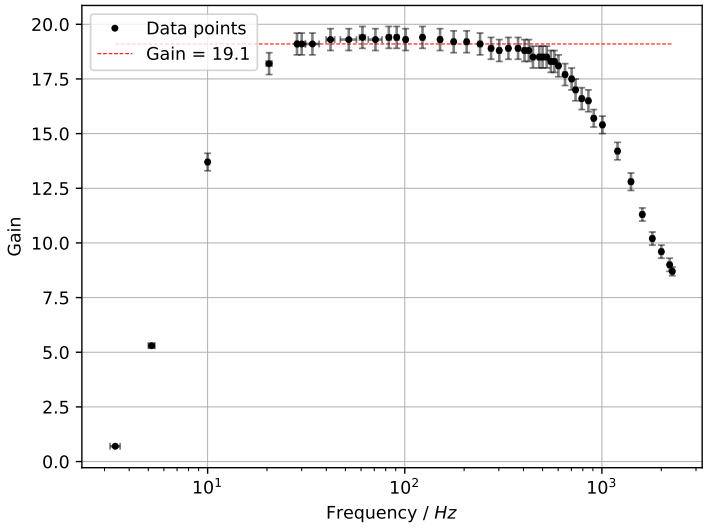

Figure 4. Graph showing gain-frequency dependence of two stage amplifier used in electric box. The region where the gain plateaus is the constant gain region which will correspond to a range of muon decay times. This is the region of decay times that will be analysed.

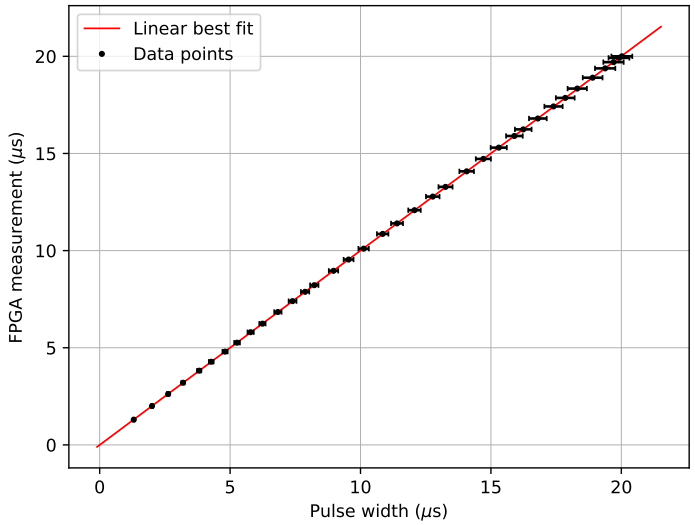

Figure 5. Graph showing linear relation between oscilloscope and FPGA timer measurements for two consecutive pulses with varying time. The linear line of best fit gives a gradient of $m = 1.0004 \pm 0.0003$ and a y-intercept of slope $c = (-0.002 \pm 0.004)$ µs.

For the gain-frequency dependence of the two stage amplifier (Figure 4), there was a constant gain (within error) for a range of frequencies from 28.4 kHz to 426 kHz. This corresponds to a constant gain region in the muon lifetimes from 2.35 µs to 35.2 µs. Due to there being a constant gain, we can now use these range of muon lifetimes to compare to simulated muon data and to calculate a more accurate mean muon lifetime value, t_μ.

For the verification on the FPGA timer (Figure 5), we obtained a value of $c = (-0.002 \pm 0.004)$ µs. This tells us that there is a small varying lag of order 10^{-3} µs between the oscilloscope and FPGA timer. This lag is around 10^3 to 10^4 smaller than time intervals measured, allowing us to have confidence in the FPGA timer readings. A value of $m = 1.0004 \pm 0.0003$ tells us that the FPGA readings will always be greater than the oscilloscopes (for $mx < c$). Taking into account uncertainty, our FPGA value will always be higher by 0.01% to 0.07% multiplied by the pulse width value. This is a systematic uncertainty in the circuit, that could later be adjusted. This allows us to then have increasing confidence that the FPGA timer displays accurate time readings.

Data run	Experiment run time (h:min:s)	HV (V)	ΔHV (V)	Threshold (V)	ΔThreshold (V)
1	87:48:23	8.2	0.1	0.40	0.01
2	87:09:17	8.9	0.1	0.59	0.01
3	90:45:46	7.5	0.1	0.60	0.07
4	86:15:35	7.8	0.1	0.48	0.01
5	88:05:22	7.8	0.1	0.42	0.07

Table 1. Experiment run times for each data run with HV and threshold voltage values used before letting the equipment collect data.

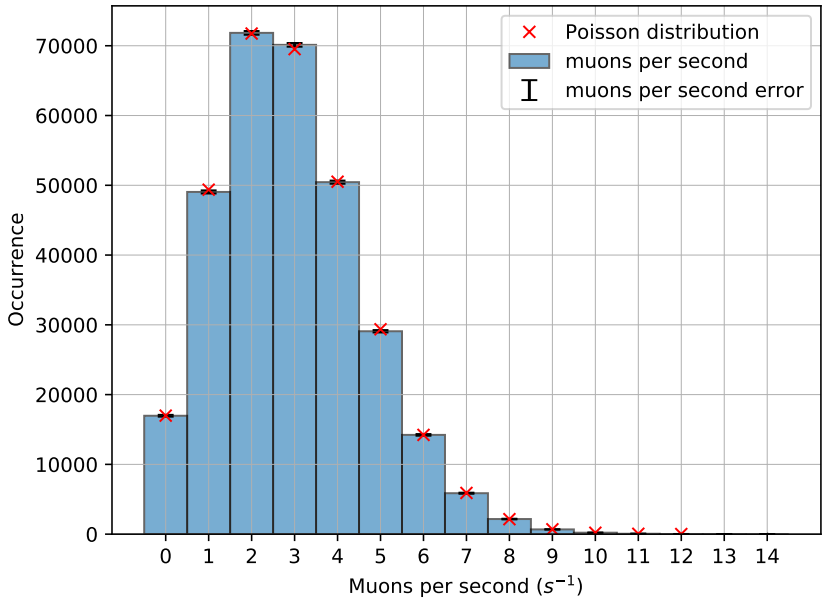

Figure 6. Incident number of muons per second for the first data run with a scintillator flux of $\Phi_S = 2.91$ muons s^{-1}. A reduced chi squared (χ_ν) analysis gives $\chi_\nu = 0.941$.

Data run	Events	Φ_S (muons s^{-1})	Reduced chi squared χ_ν
1	2754	2.91	0.941
2	2951	3.01	0.579
3	1961	2.47	0.538
4	3810	3.37	1.02
5	4742	3.66	0.707

Table 2. Total number of decay events measured for each data run with the corresponding scintillator flux values and values of a reduced chi squared analysis on the experimental data compared to a theoretical Poisson distribution.

In Table 1 the chosen HV and threshold voltages can be seen with their respective scintillator fluxes in Table 2. For the first two data runs we tried to obtain a scintillator flux value around the initial muon flux, and for the third week we used a lower scintillator flux to see whether there would be a significant difference in the muon decay times obtained. The same idea was applied to the fourth data run but with a higher scintillator flux. However, for the fifth data run, we used an improved value for the muon flux from our ongoing simulation (see Appendix A), hence why the scintillator flux and total number of events is much higher.

As we are measuring muon decay times, we expect the number of incident muons per second to follow a Poisson distribution, similar to radioactive decay. As can be seen in Figure 6, the first data run closely follows a Poisson distribution and can be quantitatively backed up by performing a reduced chi squared analysis [5] which outputs a value of $\chi_\nu = 0.941$ (Table 2 contains all reduced chi squared values). A value of $\chi_\nu \approx 1$ for data runs 1 and 4 suggest that the Poisson distribution is a good fit. Data runs 2, 3, and 5 deviate more towards a reduced chi squared value of zero, however they are still relatively close to a value of one, allowing us to have confidence that the Poisson distribution is a good fit. As we now know that the incident number of muons per second follows a Poisson distribution, we can use Poisson statistics to find the error in each bin height. Poisson statistics state that $\sigma_i = \sqrt{N_i}$ where σ_i is the error in each respective bin i, with N_i occurrences. In addition, since our data follows a Poisson distribution we are more confident that we are actually measuring muon decays.

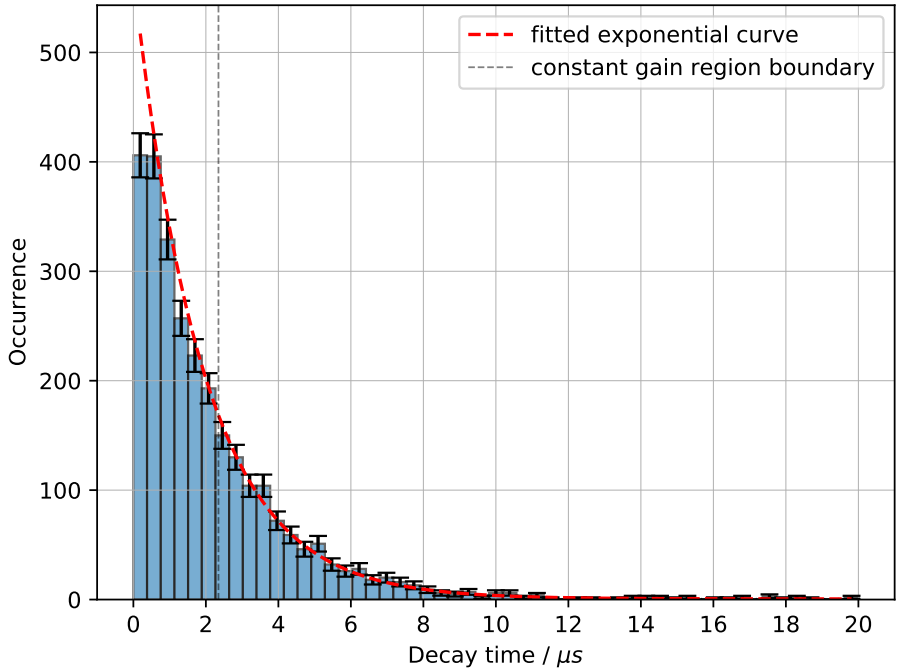

Figure 7. Muon decay data from the first data run fitted with an exponential curve using python's curve_fit function in the constant gain region. The python curve_fit function outputs values of: $A = 570 \pm 44$, $B = 0.5 \pm 0.2$ and $t_\mu = 1.92 \pm 0.07$. The optimal number of bins for the decay time histograms was chosen by using the square root method where the number of bins is equal to $\lceil \sqrt{N} \rceil$. Where N is the total number of events for each data run shown in Table 2.

Data run	A	Δ(A)	B	Δ(B)	t_μ (µs)	Δ(t_μ) (µs)	χ_ν
1	570	44	0.5	0.2	1.92	0.07	0.702
2	485	36	0.4	0.2	2.13	0.08	0.823
3	392	37	0.5	0.3	2.1	0.1	0.822
4	620	32	0.5	0.3	2.06	0.05	0.481
5	599	43	0.8	0.3	2.15	0.07	1.06

Table 3. Optimised values from pythons curve_fit function for constants A, B, and the average muon lifetime t_μ with a reduced chi squared analysis for all five data runs. The uncertainties in the parameter values are outputted by the pyhton's curve_fit function once The accepted value of muon lifetime is $\tau^+ = (2.1969811 \pm 0.0000022)$ µs [1].

Once the muon decay time data had been extracted, the decay times within the constant gain range (from 2.35 µs to 35.2 µs) were fitted with an exponential function of the form $Ae^{-\frac{t}{t_\mu}} + B$ which resembles the characteristic behaviour of muon decay from (1.3). This was achieved by using python's curve_fit function which takes the exponential fit above, with guess parameters, and fits it to the muon decay time data. The curve_fit function

does this by optimising the guess parameters (A, B and t_μ) such that it finds the minimum chi squared between the decay time data and the exponential fit. The value of the constant A represents the scaling of the exponential along the y-axis whilst the constant B represents a background measurement where an initial muon hits the scintillator producing a signal, then right after (before the FPGA reset) a second muon hits the scintillator before the first decays, producing a second signal. This background is random and has an equal probability of happening at any time.

For the first four data runs the background constant (B) seems to be around 0.5 suggesting that there is only a small number of background measurements; around 1 for every two bins. For the fifth data run, with an improved scintillator flux, there was a higher number of background measurements; this is due to there being more events compared to the other four data sets (as seen on Table 2).

From Table 3, the accepted positive muon lifetime value τ^+ only falls into the one sigma level for data runs 2, 3, and 5 with the latter being the most accurate and precise of the three. This makes sense as the fifth data run has the greatest number of muon decay events, meaning it has a greater sample size, therefore better representing the mean muon lifetime we are trying to obtain. The fourth data run falls in the 3 sigma level and the 1st data run has greater than 3 sigma levels. This could be due to the first and fourth data runs detecting more negative than positive muons, therefore making the muon lifetime value lower.

As recited in the theory (1.2), there are two methods of negative muon decay, either via spontaneous decay or muon capture. Where the decay time of muon capture is what makes the negative muon lifetime lower than the positive muon lifetime. Muon capture is proportional to Z^4 [7] where Z is the atomic number of the material of the scintillator. According to the muon physics manual [8] the material used in our scintillator can be approximated to carbon ($Z = 6$), where we can then use a value of negative muon lifetime of $\tau^- = (2.043 \pm 0.003)$ µs [9]. Data run 1 has a lifetime value lower than the negative lifetime value stated above. This suggests that data run one has been affected by an external factor such as an equipment error, or background decay of another particle that is shorter than τ^-. Measuring another particle with a lower lifetime than τ^- would skew the decay time data to the lower lifetime values, making the exponential fit look more sharp. This is why the background constant B doesn't change compared to the other data runs, as measuring other particle decays with a shorter lifetime doesn't have a universal effect, instead it skews the data. It is also possible this may have also been due to some other cosmic activity during that time.

Data run	$\frac{G_F}{(\hbar c)^3} \times 10^5$ (GeV^{-2})	$\Delta\frac{G_F}{(\hbar c)^3} \times 10^5$ (GeV^{-2})
1	1.24	0.02
2	1.18	0.02
3	1.18	0.03
4	1.20	0.01
5	1.17	0.02

Table 4. Fermi coupling constant values calculated from the average muon lifetimes using (1.4). The accepted value of the Fermi coupling constant is $\frac{G_{Facc}}{(\hbar c)^3} = (1.1663787 \pm 0.0000006) \times 10^{-5}$ GeV^{-2} [10].

Similarly to the muon lifetime analysis, the accepted Fermi coupling constant value falls in the 1 sigma level for data runs 2, 3, and 5. In addition to this, the above data runs are reliable with uncertainties equal to 1.7%, 2.5%, and 1.7% of their values respectively. The measurements also deviate by small amounts of 1.2%, 1.2%, and 0.3% from the accepted value respectively. This gives us confidence that for data runs 2, 3 and 5 we were measuring muon decays to a good degree of accuracy and precision, especially for the latter data run. Data run one is at a 4 sigma level away from the accepted value which is expected as suspect there is an external factor affecting the measurements made. Data run four has a high precision as its uncertainty is equal to 0.8% of the obtained value, however it lacks in accuracy as it also lies at the 4 sigma level and deviates by 2.9% of the accepted value.

5 Conclusion

The muon lifetime values for all data runs are lower than the accepted positive muon lifetime $\tau^+ = (2.1969811 \pm 0.0000022)$ µs [1] due to the interference of negative muons, where the negative muon lifetime $\tau^- = (2.043 \pm 0.003)$ µs [9] is smaller due to the event of muon capture. This shift of lifetimes then carries over to the Fermi coupling constant where all of the experimentally determined values are higher then the accepted value of $\frac{G_{Facc}}{(\hbar c)^3} = (1.1663787 \pm 0.0000006) \times 10^{-5}$. Overall, the most precise and accurate result came from the fifth data run which had an improved scintillator flux value from the simulation (see Appendix A). A value of $\frac{G_{Facc}}{(\hbar c)^3} = (1.17 \pm 0.02) \times 10^{-5}$ GeV^{-2} was obtained for the fifth data run which deviates by 1.7% from the accepted value and has an uncertainty which is 0.8% of the value obtained. However, the first data run deviated significantly from the accepted Fermi coupling constant value. We suspect this could have been due to equipment error, another particle being detected which could lower the average decay time or an external event such as some other cosmic activity.

Future improvements for this experiment would include detecting muons for a longer amount of time. Doing this would increase our sample size, allowing our data better represent the muon lifetime we are trying to measure. This will also decrease the statistical uncertainty in each bin due to randomness in the muon decay times for a low number of events. Another improvement would be to eliminate the systematic uncertainty in the FPGA timer in order to obtain more accurate muon decay time readings. This could be achieved by using the line of best fit found earlier. In addition to this, the correction factor from the simulation could be used to calculate a new scintillator flux. This will lead to a greater scintillator flux meaning the data will have a greater sample size. Lastly, a final improvement for the experiment would be to place a another spherical shell-shaped scintillator that encloses the current one being used. This would allow us to eliminate the background event where an initial muon hits the scintillator producing a signal, then right after (before the FPGA reset) a second muon hits the scintillator before the first decays, producing a second signal. This is because when this happens the two muons will have to pass through the spherical shell-shaped scintillator making a 'decay measurement' which can then be removed from the cylindrical scintillator decay measurements as we will know what time this happens at.

A Simulation

After the fourth data run we worked on building a simulation in order to determine a correction factor that will improve the initial flux estimate ($\Phi_{est} = 2.95$ muons s^{-1}) by taking into account muons that enter at a zenith angle other than zero and can hit both the top and side of the detector. Note that the intensity of muons at the ground as a function of zenith angle θ_Z is [1]:

$$I = I_0 \cos^2(\theta_Z) \tag{A.1}$$

where I_0 is a normalisation factor.

The simulation works by generating muons randomly on a 2-dimensional square emission plane (at an arbitrary height z) centred above the detector (cylindrical object centred at x,y = 0 representing the scintillator) with generated velocity components. The θ-components of the muon velocities are generated using a Monte Carlo simulation that generates θ-components based on (A.1) using the Monte Carlo Von Neumann rejection technique. These muons are then fired from random positions on the 2D square plane with respective Monte Carlo simulated velocities. The simulation then detects the number of muons that have hit the top and the side of the detector in order to determine a correction factor. The correction factor is determined by:

$$c_{corr} = \frac{\Phi_{top} + \Phi_{side}}{\Phi_{top}} \tag{A.2}$$

Where Φ_{top} and Φ_{side} are the respective top and side fluxes of the detector. Once a correction factor has been found, a new improved flux value can then be calculated:

$$\Phi_{imp} = c_{corr}\Phi_{est} \tag{A.3}$$

Where Φ_{imp} is the new improved muon flux value.

The simulation detects whether a muon has hit the top or side of the detector by splitting it into equally spaced 2D slices parallel to the the xy-plane (also parallel to the 2D muon emission plane). Muons hitting the top of the detector will hit the top slice, whilst muons hitting the side of the detector will hit one of the other slices in the detector. The optimal number of slices in the detector is found by calculating the angle between detector slices $\phi(S)$, and the minimum angle of approach for a muon coming from the side of the emission plane to the detector $\theta_{min}(S)$; where both are functions of the slice number S. It then finds the minimum slice number for which a muon can't go through the detector without being detected, satisfying the following equality $\phi < \theta_{min}$.

One can verify whether a muon hits a slice by finding where the vector line representing the muons trajectory from the emission plane intersects the slice plane (infinitely big plane at the same height and parallel to the slice). A muon hitting the detector will then satisfy $x^2 + y^2 \leq r^2$, where x and y are the intersection coordinates of the vector line with the slice plane and r is the radius of the detector ($r = 7.5$ as units of cm are used).

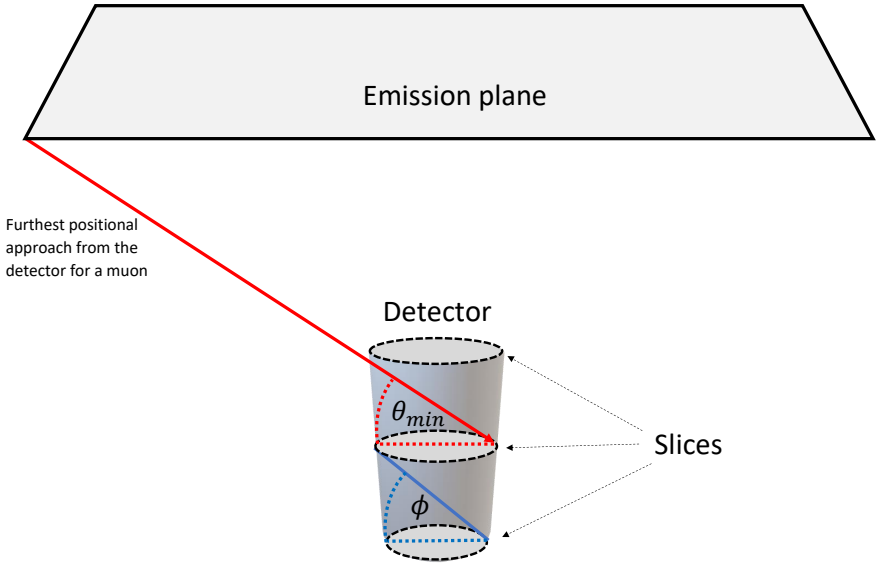

Figure 8. Diagram of simulation with an emission plane, detector split into equally spaced slices, and a representation of angles θ_{min} and ϕ. In this case the number of slices would have to increase as there is a possibility that a muon emitted from the emission plane can pass through the slices undetected (as $\theta_{min} < \phi$).

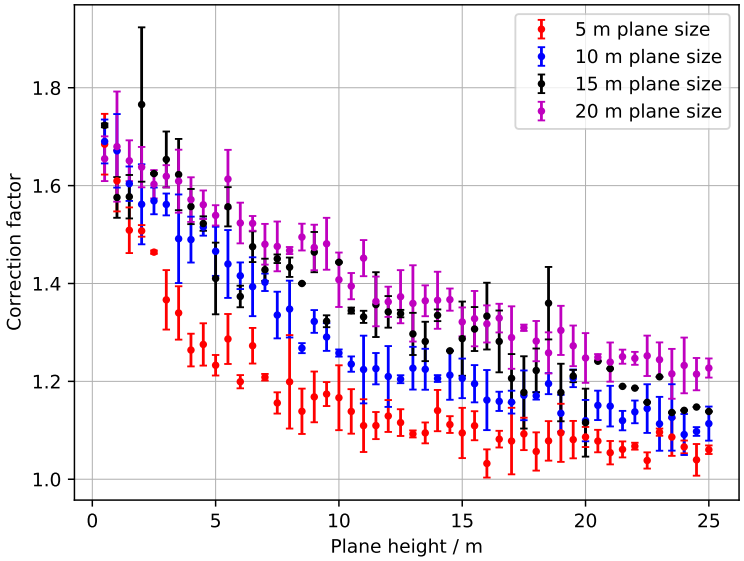

Figure 9. Simulation results for increasing plane sizes with varying heights. This was the first approach we took towards finding an improved muon flux Φ_{imp}, which we took to be the correction factor for the 20 m plane size at the 25 m plane height. This outputs a value of $c_{corr} = 1.21 \pm 0.02$.

The first approach we took towards using the simulation was to increase the plane size with varying plane heights. We hypothesised that as the plane size increases, the correction factor will converge for big heights. In Figure 9, a small convergence can be seen, however bigger plane sizes would be needed in order to confirm this. For simulating the bigger plane sizes at greater heights, more muons were needed thus making the simulation longer. This is because if you run the simulation multiple times for a constant plane size and height, the top (Φ_{top}) and side (Φ_{side}) flux values will fluctuate due to the randomness of the muon emission coordinates and velocities, thus giving random fluctuations in the correction factor. The only way of decreasing this fluctuation or uncertainty, is to increase the number of muons being emitted thus making the simulation longer. In Figure 9, three simulation runs were applied to every plane size (except 15 m, where there were 2 runs) and the uncertainty in the correction factor was taken to be the standard deviation of the three correction factor values.

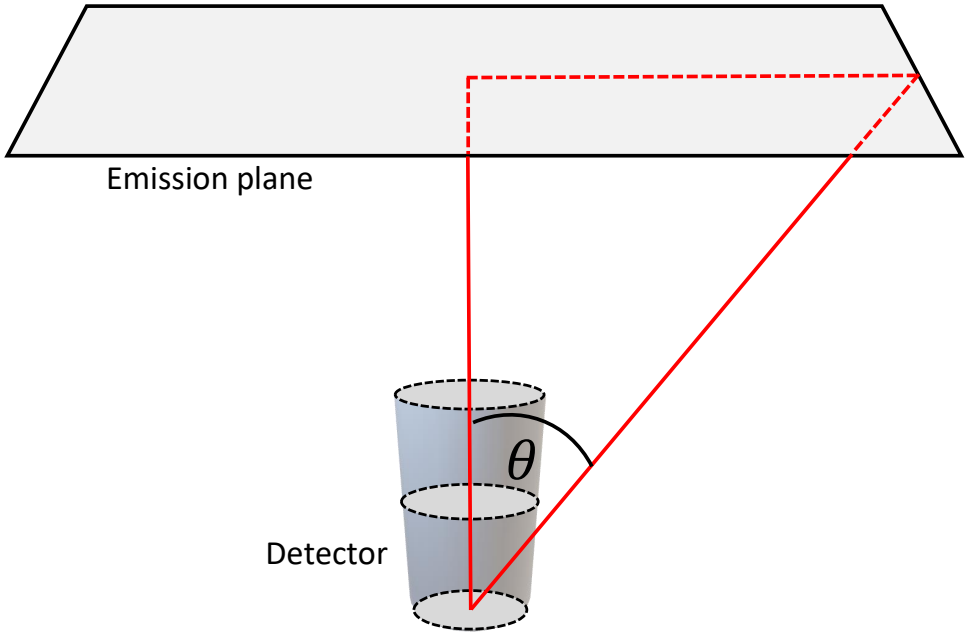

Figure 10. Diagram depicting the angle θ between the detector and emission plane that was used in the second approach of muon simulation in order to obtain an improved correction factor c_{corr}.

Towards the end of the first approach we realised that by increasing the emission plane height for varying plane sizes, we were forcing more muons to hit the top of the detector as the angle θ between the centre of the detector and the side of the emission plane (Figure 10) was decreasing with an increasing plane height. This meant that we were forcing the simulation to give an underestimate in the correction factor as there was going to be a greater top flux compared to the side flux. A way of fixing this would be to consider higher θ values, however that would require us going to bigger heights making the simulation

longer. We had only realised this just before the fifth data run, so we decided to use this improved correction factor (using (A.3)) of $\Phi_{imp} = (3.57 \pm 0.06)$ muons s^{-1} as our scintillator flux Φ_S in data run 5.

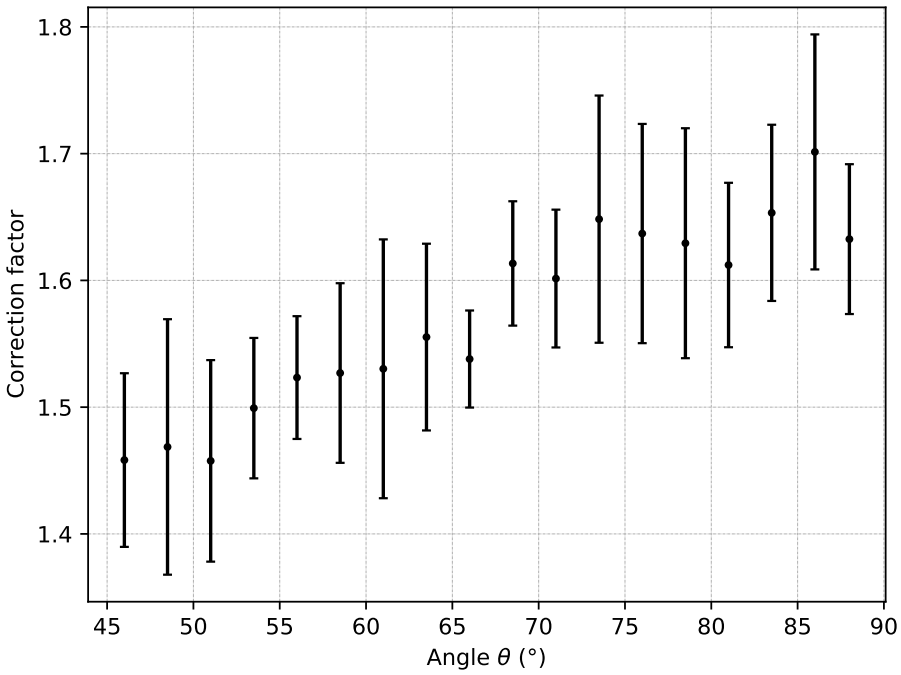

Figure 11. Correction factor for varying θ values in the range of 46 to 88 degrees. The plane height was kept at a constant value of 1 m.

For the second approach of the muon simulation, we considered varying angles. In this approach we hypothesised that to simulate the atmosphere as a 2D plane in a simulation, we would need the angle θ to be very large (close to 90 degrees). This is because the Earths atmosphere, although at a very large height, also has a curvature such that muons can approach the detector at angles close to 90 degrees (this event is very unlikely to occur). For each angle, 10 correction factors were determined and averaged, and the uncertainty was taken to be the standard deviation.

As can be seen in Figure 11, the correction factor converges for an angle that tends to a value of 90 degrees. This new correction factor is taken to be the average of the 86 and 88 degree correction factors, and outputs a value of $c_{corr} = 1.7 \pm 0.1$. This improved correction factor then outputs a value of $\Phi_{imp} = (4.9 \pm 0.3)$ muons s^{-1} for improved muon flux when plugged into A.3.

References

[1] P.A. Zyla et al. (Particle Data Group). *Review of particle physics*. Prog. Theor. Exp. Phys. 2020, 083C01 (2020).

[2] T.V. Ritbergen, R.G. Stuart. *On the Precise Determination of the Fermi Coupling Constant from the Muon Lifetime*. Nucl.Phys. B564 (2000) pg.343-390.

[3] S.H. Neddermeyer and C.D. Anderson. *Note on the Nature of Cosmic Ray Particles*. Phys.Rev. 51 (1937) pg.884-886

[4] J.C. Street and E.C. Stevenson. *New Evidence for the Existence of a Particle of Mass Intermediate Between the Proton and Electron*. Phys.Rev. 52 (1937) pg.1003-1004

[5] I. G. Hughes and T. P. A. Hayes. *Measurements and their Uncertainties*. Oxford: Oxford University Press, 2010. pg. 107

[6] Coan T, Liu T, Ye J. *A compact apparatus for muon lifetime measurement and time dilation demonstration in the undergraduate laboratory*. Am. J. Phys. 74 (2006) pg. 161-164

[7] NE. Fermi, E. Teller. *The Capture of Negative Mesotrons in Matter*. Phys. Rev. 72, (1947) pg.399

[8] T. E. Coan, J. Ye. *Muon Physics*.

[9] R. A. Reiter et al. *Precise Measurements of the Mean Lives of μ^+ and μ^- Mesons in Carbon*. Phys. Rev. Lett. 5

[10] P Mohr, B Taylor, D Newell. *CODATA Recommended Values of the Fundamental Physical Constants: 2014*. J. Phys. Chem. Ref. Data 45, 043102 (2016)